

See discussions, stats, and author profiles for this publication at: <https://www.researchgate.net/publication/257529719>

Quantification of chromatin condensation level by image processing

Article in Medical Engineering & Physics · October 2013

DOI: 10.1016/j.medengphy.2013.09.006 · Source: PubMed

CITATIONS

5

READS

272

3 authors:



Jerome Irianto

University of Pennsylvania

56 PUBLICATIONS 785 CITATIONS

[SEE PROFILE](#)



David Lee

Queen Mary, University of London

186 PUBLICATIONS 5,389 CITATIONS

[SEE PROFILE](#)



Martin M Knight

Queen Mary, University of London

112 PUBLICATIONS 2,699 CITATIONS

[SEE PROFILE](#)

Some of the authors of this publication are also working on these related projects:



Mechano-regulation of genome function to direct stem cell fate [View project](#)



TOPOGRAPHY OF CALCIUM PHOS [View project](#)



Contents lists available at ScienceDirect

Medical Engineering & Physics

journal homepage: www.elsevier.com/locate/medengphy



Technical note

Quantification of chromatin condensation level by image processing

Jerome Irianto*, David A. Lee, Martin M. Knight

Institute of Bioengineering, School of Engineering and Materials Science, Queen Mary, University of London, London, United Kingdom

ARTICLE INFO

Article history:

Received 22 March 2013
Received in revised form 3 July 2013
Accepted 9 September 2013

Keywords:

Chromatin condensation
Image quantification
Image processing
MATLAB
Sobel edge detection algorithm

ABSTRACT

The level of chromatin condensation is related to the silencing/activation of chromosomal territories and therefore impacts on gene expression. Chromatin condensation changes during cell cycle, progression and differentiation, and is influenced by various physicochemical and epigenetic factors.

This study describes a validated experimental technique to quantify chromatin condensation. A novel image processing procedure is developed using Sobel edge detection to quantify the level of chromatin condensation from nuclei images taken by confocal microscopy. The algorithm was developed in MATLAB and used to quantify different levels of chromatin condensation in chondrocyte nuclei achieved through alteration in osmotic pressure. The resulting chromatin condensation parameter (CCP) is in good agreement with independent multi-observer qualitative visual assessment. This image processing technique thereby provides a validated unbiased parameter for rapid and highly reproducible quantification of the level of chromatin condensation.

© 2013 IPEM. Published by Elsevier Ltd. All rights reserved.

1. Introduction

The cell nucleus is a double membrane bound organelle containing genetic information stored in form of deoxyribonucleic acid (DNA). Many essential functions take place in the nucleus, such as the initial steps of gene expression including messenger ribonucleic acid (mRNA) transcription, DNA replication, repair, and recombination, as well as the production of ribosomal RNA (rRNA). The DNA in a eukaryotic cell nucleus is grouped into chromosomes, each containing a linear DNA molecule associated with proteins, such as the histones, that fold and pack the DNA into a more compact structure called chromatin.

Chromatin can be classified into heterochromatin or euchromatin, based on the condensation level during interphase. Euchromatin consists of less condensed chromatin, which is typically transcriptionally active [1] and often located towards the interior of the nucleus. By contrast, heterochromatin is more condensed, generally associated with gene silencing [2,3] and often located at the nuclear periphery, around the nucleolus, and as patches throughout the nucleoplasm [4,5]. Chromatin condensation often correlates with the level of cell differentiation with a more decondensed chromatin organisation found in stem cells compared to the localised condensed regions found in the nuclei of differentiated cells [6]. Chromatin also condenses prior to cell division and apoptosis [7]. Additionally, chromatin condensation

can be induced by physicochemical stimuli, such as the addition of multivalent cations [8,9], and alteration in osmolality [10–13].

It is therefore useful to be able to assess the degree of chromatin condensation using quantitative parameters. In most previous studies, chromatin condensation is typically assessed qualitatively by visual observation of microscopic images of the nucleus. Meanwhile, some studies assessed the level of chromatin condensation quantitatively via Fluorescence Recovery After Photobleaching (FRAP) analysis of H2B [14] or HP1 mobility [15], a protein present in condensed chromatin [16]. Here, we describe a novel procedure to quantify the level of chromatin condensation by processing of fluorescence or confocal microscopy images based on an edge detection algorithm.

2. Methods and results

2.1. Cell preparation

Primary bovine chondrocytes were isolated from full depth cartilage of the metacarpo-phalangeal joints of freshly sacrificed eighteen to twenty four months old bovine via a series of enzymatic digestions, as previously described [17]. Freshly isolated chondrocytes were seeded onto 175 cm² culture flasks (8×10^6 cells/flask) and cultured for 5 days in low glucose Dulbecco's modified Eagle's medium (DMEM) to ensure the adhesion of the cells. The media was supplemented with 20% foetal calf serum (FCS), 20 mM HEPES, 100 U ml⁻¹ penicillin, 0.1 mg ml⁻¹ streptomycin, 2 mM L-glutamine and 0.85 mM L-ascorbic acid (all from Sigma–Aldrich, Dorset, UK). For the H5 murine chondrocyte cell lines [18], the cells were also seeded at the same density onto 175 cm² flasks and cultured in

* Corresponding author. Tel.: +44 (0)20 7882 8868.
E-mail address: j.irianto@qmul.ac.uk (J. Irianto).

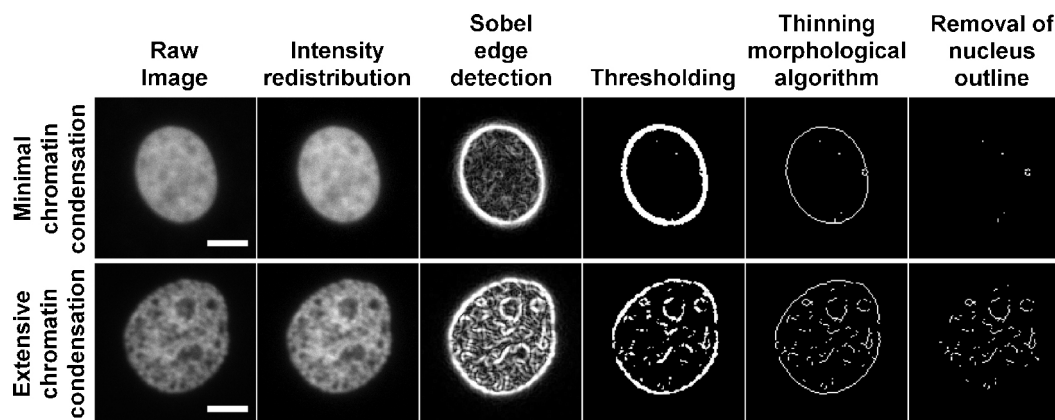


Fig. 1. Images of two separate nuclei with minimal (top) and extensive (bottom) chromatin condensation, showing the results of each image processing step leading to the calculation of the chromatin condensation parameter (CCP) (bar: 5 μm). From this quantification, the nucleus with minimal condensed chromatin has a CCP of 0.16%, compared to 4.86% for the extensively condensed chromatin.

DMEM/F12 media supplemented with 15 mM HEPES (Invitrogen, Paisley, UK) and 10% FCS. The cultured cells were trypsinised and seeded onto FCS coated coverslips, housed in 24 well plates, with a seeding density of 3×10^4 cells cm^{-2} .

In order to obtain nuclei with different degree of chromatin condensation, the cells were subjected to osmotic challenge by incubation medium with osmolalities in the range 100–800 mOsm kg^{-1} for 15 min to allow for chromatin reorganisation [10]. We have previously shown that this produces a rapid alteration in chromatin condensation [13]. The standard culture media had an osmolality of 320 mOsm/kg, which was increased by the addition of D-Mannitol (Sigma–Aldrich) and was reduced by the dilution with sterile distilled water.

2.2. Fluorescent staining and confocal microscopy

Cells were washed with osmotically balanced PBS and fixed by incubation in osmotically balanced fixative, 1% glutaraldehyde (Agar Scientific, Stansted, UK) buffered with 8 mM sodium cacodylate (Sigma–Aldrich), for 30 min. The specimens were subsequently washed with PBS and stained with 8 μM Hoechst 33342 (Sigma–Aldrich) for 15 min in 37 °C. The specimens were washed with sterile distilled water and mounted onto glass slides by using Prolong Gold (Invitrogen, Paisley, UK). The chondrocyte nuclei were imaged using confocal microscopy (Leica TCS SP2, Leica Microsystems GmbH, Wetzlar, Germany), using a $63\times/1.4\text{NA}$ oil immersion objective at a resolution of 46.5 nm/pixel (512 \times 512 pixels per image) and an imaging period of 7.68 s/image⁻¹. Intensity levels for each pixel were recorded on an 8 bit scale (0–255).

2.3. Quantification of chromatin condensation parameter

The condensation of chromatin increases the number of distinct spaces within the nucleus. This is detected by the Sobel edge detection algorithm [19]. Thus, measuring the density of edges within the nucleus, normalised to its cross-section area, gives a measure of the level of chromatin condensation defined as the chromatin condensation parameter (CCP).

In order to calculate this parameter, images of nuclei obtained by confocal microscopy were subjected to a series of transformations as shown in Fig. 1 for two separate nuclei with different degrees of chromatin condensation. First, to standardise the image, the intensity profile was redistributed by dividing each pixel intensity by the maximum intensity of the image and multiplying by 255 (the maximum intensity for 8-bit image). This was followed by the edge detection procedure using Sobel edge detection, a gradient based

algorithm where a gradient of consecutive pixels is approximated in X and Y direction. Sobel edge detection uses two 3×3 kernels to approximate the gradients between a pixel and the 8 surrounding pixels and its principle can be described as follow:

$$S_x = \begin{bmatrix} +1 & 0 & -1 \\ +2 & 0 & -2 \\ +1 & 0 & -1 \end{bmatrix} \quad \text{and} \quad S_y = \begin{bmatrix} -1 & -2 & -1 \\ 0 & 0 & 0 \\ +1 & +2 & +1 \end{bmatrix} \quad (1)$$

$$G_x = S_x \times I \quad (2)$$

$$G_y = S_y \times I \quad (3)$$

$$G = \sqrt{G_x^2 + G_y^2} \quad (4)$$

where S_x is Sobel kernel for the approximation of gradient in X direction, S_y is Sobel kernel for the approximation of gradient in Y direction, G_x is the approximated gradient in X direction, G_y is the approximated gradient in Y direction, I is the target image matrix and G is the approximated gradient magnitude. The resulting gradient magnitude is then used to represent the processed pixel of interest in the target image. This process is repeated for each pixel within the target image. The final step of the Sobel algorithm produces a new image showing the level of edges based on the gradient magnitude.

Chromatin condensation increases the number of distinct spaces within the nucleus, creating sudden dips of intensity across the nucleus image. These sudden dips of intensity are detected by the Sobel algorithm as strong edges. Hence, the increase of chromatin condensation level is directly correlated to the higher number of strong edges within the nucleus. The Sobel image produced was thresholded to acquire the strong edges.

In order to count the number of strong edges, the thresholded Sobel image underwent a thinning algorithm [20], which transforms an entity within the image into a single pixel thickness entity. Due to the marked difference in intensity between the imaged nucleus and the background, the Sobel filter generates an artificial edge at the boundary of the nucleus. This artificial edge should be removed, as they do not represent the level of chromatin condensation. With the removal of the nucleus outline, the number of edges was measured and dividing by the area of the nucleus gives the edge density, i.e. the CCP.

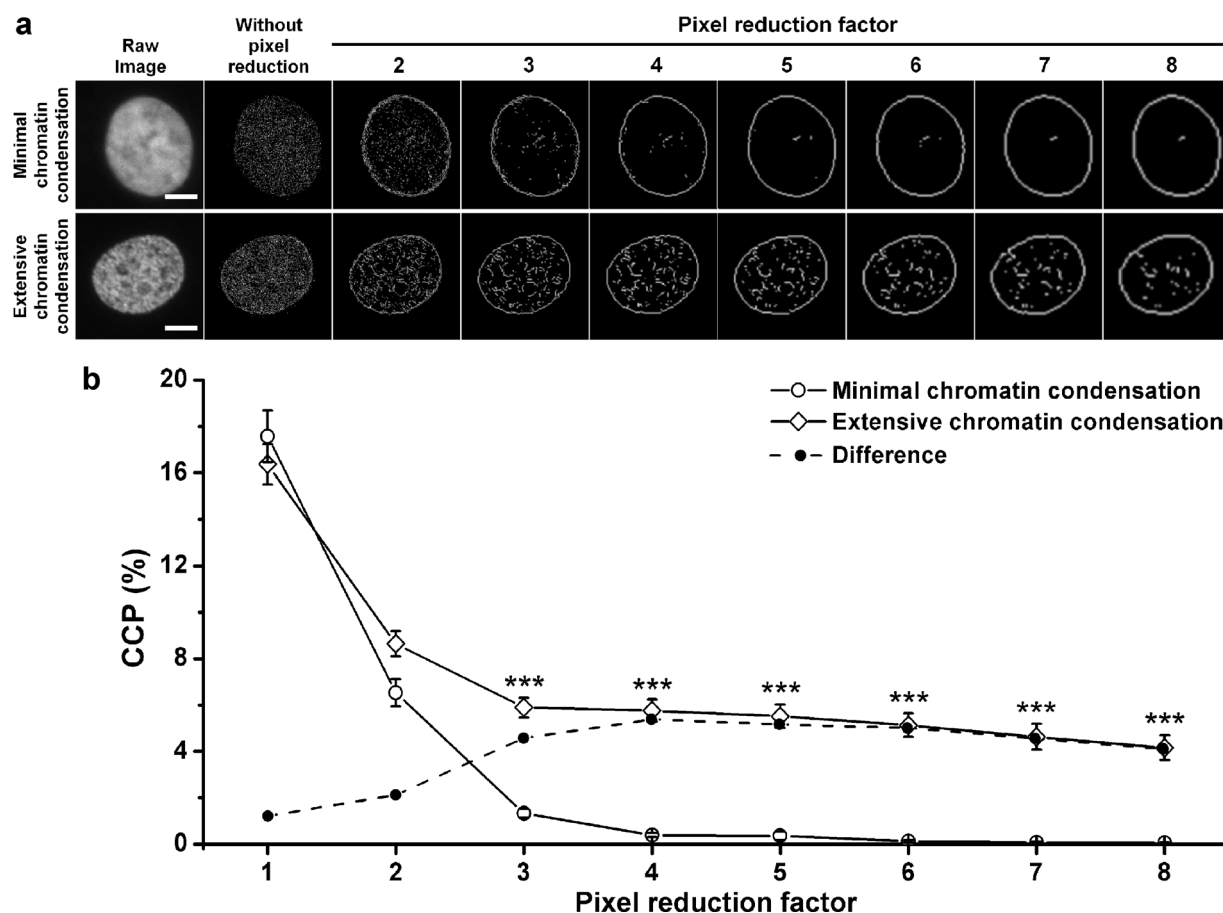


Fig. 2. The influence of pixel reduction factor on CCP. Confocal images of nuclei showing minimal (top) and extensive (bottom) chromatin condensation and the effect of pixel reduction factors (2–8) followed by Sobel edge detection, thresholding and thinning (a) (bar: 5 μ m). The CCP measured from the nuclei with minimal and extensive chromatin condensation ($n = 20$ nuclei per group) is shown against the pixel reduction factor (b) (***) ($p < 0.001$). Values represent the mean with error bars indicating standard error.

2.4. Pixel reduction factor

As the Sobel edge detection algorithm only considers the 8 surrounding pixels to approximate the gradient magnitude, it is very sensitive to intensity fluctuation between the neighbouring pixels such that the edges produced do not represent the level of chromatin condensation. Indeed preliminary studies found this to occur with the images acquired in this study when subjected to Sobel edge detection (Fig. 2a).

To resolve this problem, images were reduced in size prior to Sobel filtering. The image reduction provided a new image, where non-overlapping groups of pixel from the original image are averaged and the mean values are represented as the pixels of the new image. For example, when a 512×512 pixels image is reduced by a pixel reduction factor of 4, each 4×4 pixel groups in the original image are averaged and the mean values are represented as the pixels of the new image, resulting in a 128×128 pixels image.

To determine the optimum pixel reduction factor, the CCP of 20 nuclei with minimal and extensive chromatin condensation were measured following image reduction with different pixel reduction factor (2–8, Fig. 2b). Fig. 2 demonstrates how increasing the pixel reduction factor reduces the sensitivity of the subsequent Sobel edge detection and hence the magnitude of the CCP. The statistical significance for each image reduction group was calculated by using one-way ANOVA followed by Bonferroni's correction. The difference in CCP for the two groups of nuclei can be clearly observed following image reduction by a factor of 3. However, the maximum difference occurred at factor 4. Based on this finding,

image reduction by a factor of 4 was chosen to be used in the quantification of chromatin condensation.

2.5. MATLAB routine

MATLAB (The MathWorks, Natick, MA) incorporated with image processing toolbox was used to apply the Sobel edge detection algorithm to the nuclei image and to measure the chromatin

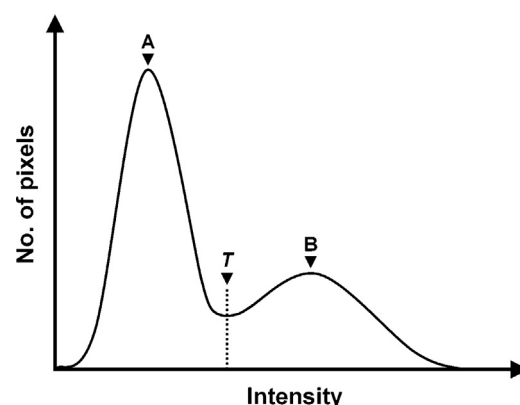


Fig. 3. Intensity histogram of a nucleus confocal image. A and B represent the local 'maxima' for background and Hoechst staining, respectively, with T being the minimum point between the two 'maxima', which was used as the threshold value in the mode thresholding method.

Table 1
The binning range of the chromatin condensation parameter reading for each bin group, including the number of nuclei registered to each group (from 640 nuclei) and the minimum, maximum and mean of the readings.

| Group | Bin range of reading | Number of nuclei | Chromatin condensation parameter | | | |
|-------|----------------------|------------------|----------------------------------|-----------------|--------|-------|
| | | | Minimum reading | Maximum reading | Mean | SEM |
| 1 | $n \leq 0.5\%$ | 171 | 0 | 0.499 | 0.200 | 0.012 |
| 2 | $0.5\% < n < 2\%$ | 148 | 0.503 | 1.991 | 1.002 | 0.034 |
| 3 | $2\% \leq n < 4\%$ | 61 | 2.006 | 3.992 | 2.977 | 0.072 |
| 4 | $4\% \leq n < 6\%$ | 55 | 4.110 | 5.960 | 5.013 | 0.078 |
| 5 | $6\% \leq n < 8\%$ | 79 | 6.010 | 7.959 | 7.005 | 0.061 |
| 6 | $8\% \leq n < 10\%$ | 56 | 8.003 | 9.953 | 9.007 | 0.079 |
| 7 | $10\% \leq n < 12\%$ | 46 | 10.011 | 11.988 | 10.828 | 0.086 |
| 8 | $12\% \leq n$ | 24 | 12.027 | 17.680 | 13.545 | 0.305 |

condensation parameter. First of all, the image was loaded into MATLAB, transforming the image into a matrix form where each element represents the intensity of the corresponding pixel. Henceforth, this image matrix is referred to as the original image matrix.

A threshold value for the original image matrix was calculated by the mode method [21], which assumes a bimodal histogram. The histogram of the image was iteratively smoothed by running it through 3×3 average filter, until there were only two local 'maxima'. The threshold intensity value (T) is the minimum point between the 'maxima', such that $y(T - 1) > y(T) \leq y(T + 1)$, where y is the number of pixels of intensity T (Fig. 3). The average filter provides a new intensity for each pixel based on the surrounding pixels in a kernel. In order to get a better outline of the nucleus, the original image matrix was then smoothened 6 times by running it through 3×3 average filter. The threshold was applied to the smoothed original image matrix, producing a binary image showing the pixels that lie above the threshold value. A hole filling algorithm [22]

was applied to the binary image to exclude the spaces within the nucleus.

At this stage, the pixels showing in the binary image represent the location of the nucleus of interest. By using the pixel location information from the binary image, the nucleus of interest on the original image matrix was extracted and moved onto a black background (intensity equal to 0). The intensity profile of the image was redistributed and the redistributed image was reduced by a factor of 4, as described above. The threshold value for the reduced image was acquired by using the mode method. The threshold value was applied to the reduced image, resulting in a binary image showing the pixels that lie above the threshold value. A hole filling algorithm was applied to the binary image to exclude the spaces within the binary image. The perimeter of the nucleus in the binary image was acquired. In order to reduce the nucleus size by one pixel following the outline of the nucleus, the perimeter image was subtracted from the binary image. The nucleus size was reduced by one pixel

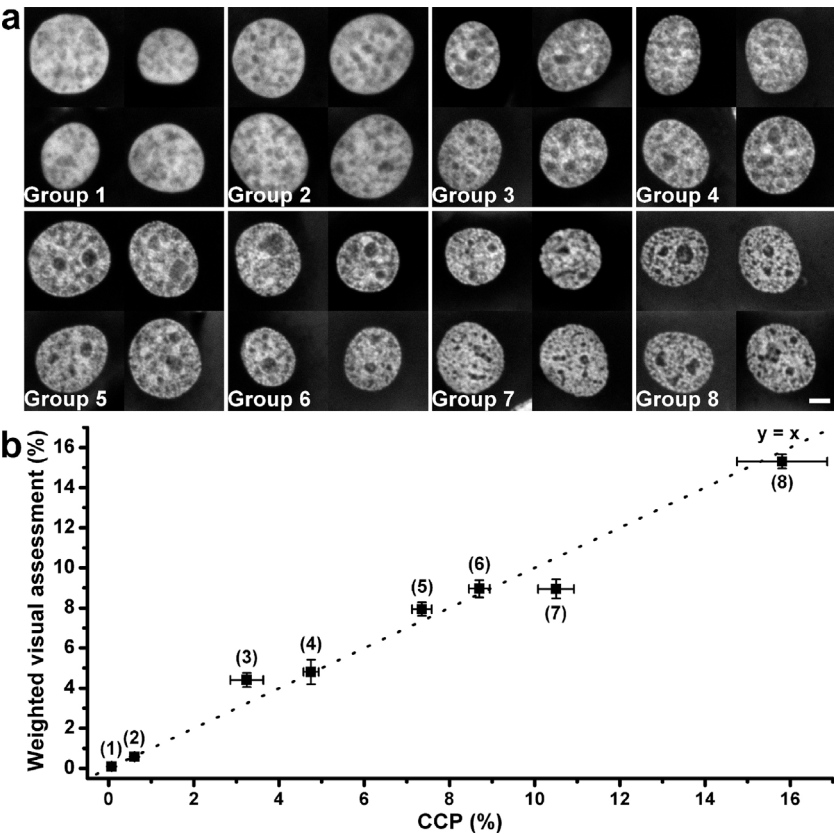


Fig. 4. The chromatin condensation parameter correlates with all independent weighted visual assessment of chromatin condensation. Representative images of monolayer primary bovine chondrocyte nuclei from each group (a) (bar: 5 μm). The CCP measured from the representative images ($n = 4$ nuclei per group) against the weighted visual assessment values ($n = 21$ inspectors per group) for each group (b), with a dotted line showing a linear relationship $y = x$. Values represent the mean with error bars indicating standard error. The number in brackets indicates the group for each data point.

again by the same procedure. At this stage, the pixels showing in the binary image represent the location of the inner part of the nucleus, where summation of the pixels from this binary image gave the area of the nucleus.

The intensity profile of the reduced image was redistributed and the Sobel edge algorithm was applied. Afterward, the Sobel image produced was thresholded and underwent the thinning morphological algorithm, as described above. The threshold value was kept constant at 0.09 for all the images processed. This value gave the best contrast between the different chromatin condensation levels for our study. By using the pixel location information from the inner part of the nucleus binary image, the processed Sobel image was extracted and moved onto a black background. Summation of the pixels from the extracted Sobel image gave the number of edges within the inner part of the nucleus. The number of edges was divided by the area of the nucleus to give the chromatin condensation parameter. This MATLAB routine is illustrated as a flow chart which can be seen in Online Resource 1 (Fig. S1).

2.6. Validation against visual assessment

The CCP was compared against a qualitative assessment by 21 independent trained observers. Images of 640 nuclei were grouped based on their CCP reading into 8 groups, with the binning range shown in Table 1. Four images from each group were chosen to represent the group (Fig. 4a). These groups of images were then sorted randomly (not based on the ascending chromatin condensation parameter order) and given to 21 independent inspectors who ranked the groups based on a visual assessment of the level of chromatin condensation. For each observer, the visual assessment ranks were weighted towards the mean of the CCP quantified from the representative images of each group. Respectively, rank 1, 2, 3, 4, 5, 6, 7 and 8 were given the value 0.07%, 0.61%, 3.24%, 4.75%, 7.35%, 8.7%, 10.5% and 15.81%. The weighted visual assessment values were averaged for each group and plotted against the chromatin condensation parameter of the corresponding group. Thus, if the inspectors gave the right ranking to a group, the weighted value will be equal to the mean reading of the group.

From Fig. 4b, most of the inspectors ranked group 1, 2 and 8 correctly. However, there was variability in the ranking of group 3–7 as indicated by the standard error. Based on the feedbacks from the inspectors, it was harder to distinguish visually between group 3 and 4, and also between group 5, 6 and 7. Generally, there is very good agreement between the chromatin condensation parameter quantified and the ranking given by the inspectors. The chromatin condensation levels of osmotically-challenged H5 murine chondrocyte cell lines were also quantified by the same algorithm (Fig. S2 in Online Resource 1). The level of chromatin condensation of H5 nuclei increases with media osmolality, which is represented by the increase of CCP.

3. Conclusions

In this study, the Sobel edge detection algorithm is utilised to quantify the level of chromatin condensation in confocal images of fluorescently labelled nuclei. The resulting CCP was validated against visual assessment on the level of chromatin condensation. Moreover, the technique provides an advantage over qualitative visual assessment in that it can be used effectively to screen large numbers of cells (e.g. $n = 640$) and thereby reveal subtle differences despite inherent variability in chromatin condensation within the sample population. In this study the nuclei were labelled with Hoechst 33342 but the method is applicable to other fluorescence labelling protocols. By developing this image processing technique, we provide a novel image analysis parameter, with freely available

MATLAB routine, to indicate the level of chromatin condensation in various types of cells.

Competing interests

None declared.

Funding

This study was supported by a Queen Mary, University of London College DTA studentship, EPSRC Platform Grant EP/E046975/1 and Human Frontiers of Science Programme grant RGP0025–2009.

Ethical approval

Not required.

Acknowledgements

The authors thank Oluwamayokun Adetoro, Zaheer Ikram, Chetan Jagadeesh and Waskito Prawira for their insight in MATLAB and image processing techniques.

Appendix A. Supplementary data

Supplementary material related to this article can be found, in the online version, at <http://dx.doi.org/10.1016/j.medengphy.2013.09.006>.

References

- [1] Hsu TC. Differential rate in RNA synthesis between euchromatin and heterochromatin. *Exp Cell Res* 1962;27:332–4.
- [2] Brown KE, Guest SS, Smale ST, Hahm K, Merckenschlager M, Fisher AG. Association of transcriptionally silent genes with Ikaros complexes at centromeric heterochromatin. *Cell* 1997;91(6):845–54.
- [3] Croft JA, Bridger JM, Boyle S, Perry P, Teague P, Bickmore WA. Differences in the localization and morphology of chromosomes in the human nucleus. *J Cell Biol* 1999;145(6):1119–31.
- [4] Alberts B, Wilson JH, Hunt T. Molecular biology of the cell. 5th ed. New York: Garland Science; 2008.
- [5] Prasanth KV, Spector DL. The cell nucleus. In: Encyclopedia of life sciences. John Wiley & Sons, Ltd.; 2005.
- [6] Francastel C, Schübeler D, Martin DI, Groudine M. Nuclear compartmentalization and gene activity. *Nat Rev Mol Cell Biol* 2000;1(2):137–43.
- [7] Kerr JF, Wyllie AH, Currie AR. Apoptosis: a basic biological phenomenon with wide-ranging implications in tissue kinetics. *Br J Cancer* 1972;26(4):239–57.
- [8] Pajewski JD, Dahl KN, Zhong FL, Sammak PJ, Discher DE. Physical plasticity of the nucleus in stem cell differentiation. *Proc Natl Acad Sci U S A* 2007;104(40):15619–24.
- [9] Sen D, Crothers DM. Condensation of chromatin: role of multivalent cations. *Biochemistry* 1986;25(7):1495–503.
- [10] Albiez H, Cremer M, Tiberi C, Vecchio L, Schermelleh L, Dittrich S, Küpper K, Joffe B, Thormeyer T, von Hase J, Yang S, Rohr K, Leonhardt H, Solovei I, Cremer C, Fakan S, Cremer T. Chromatin domains and the interchromatin compartment form structurally defined and functionally interacting nuclear networks. *Chromosome Res* 2006;14(7):707–33.
- [11] Martin RM, Cardoso MC. Chromatin condensation modulates access and binding of nuclear proteins. *FASEB J* 2010;24(4):1066–72.
- [12] Finan JD, Leddy HA, Guilak F. Osmotic stress alters chromatin condensation and nucleocytoplasmic transport. *Biochem Biophys Res Commun* 2011;408(2):230–5.
- [13] Irianto J, Swift J, Martins RP, McPhail GD, Knight MM, Discher DE, Lee DA. Osmotic challenge drives rapid and reversible chromatin condensation in chondrocytes. *Biophys J* 2013;104(4):759–69.
- [14] Chalut KJ, Höpfner M, Lautenschläger F, Boyde L, Chan CJ, Ekpenyong A, Martinez-Arias A, Guck J. Chromatin decondensation and nuclear softening accompany Nanog downregulation in embryonic stem cells. *Biophys J* 2012;103(10):2060–70.
- [15] Cheutin T, McNairn AJ, Jenuwein T, Gilbert DM, Singh PB, Misteli T. Maintenance of stable heterochromatin domains by dynamic HP1 binding. *Science* 2003;299(5607):721–5.
- [16] Arney KL, Fisher AG. Epigenetic aspects of differentiation. *J Cell Sci* 2004;117(Pt 19):4355–63.
- [17] Leef D.A., Knight MM. Mechanical loading of chondrocytes embedded in 3D constructs: in vitro methods for assessment of morphological and metabolic response to compressive strain. *Methods Mol Med* 2004;100:307–24.

- [18] van Beuningen HM, Stoop R, Buma P, Takahashi N, van der Kraan PM, van den Berg WB. Phenotypic differences in murine chondrocyte cell lines derived from mature articular cartilage. *Osteoarthritis Cartilage* 2002;10(12):977–86.
- [19] Sobel I. Neighborhood coding of binary images for fast contour following and general binary array processing. *Comput Graph Image Process* 1978;8(1):127–35.
- [20] Lam L, Lee SW, Suen CY. Thinning methodologies – a comprehensive survey. *IEEE Trans Pattern Anal Mach Intell* 1992;14(9):869–85.
- [21] Prewitt JM, Mendelsohn ML. The analysis of cell images. *Ann N Y Acad Sci* 1966;128(3):1035–53.
- [22] Soille P. *Morphological image analysis: principles and applications*. Berlin: Springer; 1999.